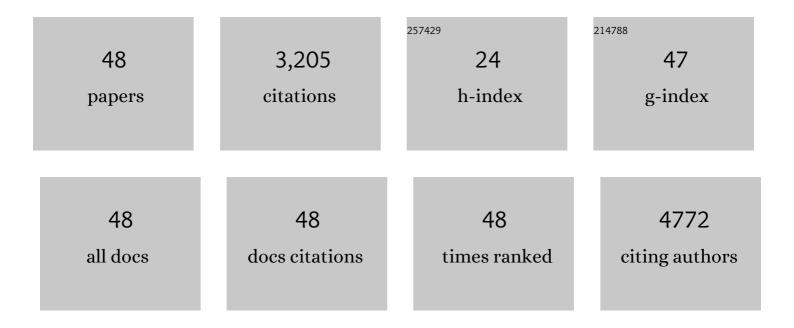
Jon Golding

List of Publications by Year in descending order

Source: https://exaly.com/author-pdf/6181225/publications.pdf Version: 2024-02-01



#	Article	IF	CITATIONS
1	The Long Non-Coding RNA H19 Drives the Proliferation of Diffuse Intrinsic Pontine Glioma with H3K27 Mutation. International Journal of Molecular Sciences, 2021, 22, 9165.	4.1	4
2	Galactose:PEGamine coated gold nanoparticles adhere to filopodia and cause extrinsic apoptosis. Nanoscale Advances, 2019, 1, 807-816.	4.6	4
3	A comparison of the radiosensitisation ability of 22 different element metal oxide nanoparticles using clinical megavoltage X-rays. Cancer Nanotechnology, 2019, 10, .	3.7	19
4	Photodynamic therapy and diagnosis: Principles and comparative aspects. Veterinary Journal, 2018, 233, 8-18.	1.7	93
5	Glycolysis inhibition improves photodynamic therapy response rates for equine sarcoids. Veterinary and Comparative Oncology, 2017, 15, 1543-1552.	1.8	13
6	Cancer-selective, single agent chemoradiosensitising gold nanoparticles. PLoS ONE, 2017, 12, e0181103.	2.5	5
7	Gold nanoparticles for cancer radiotherapy: a review. Cancer Nanotechnology, 2016, 7, 8.	3.7	329
8	Engineered neural tissue with aligned, differentiated adipose-derived stem cells promotes peripheral nerve regeneration across a critical sized defect in rat sciatic nerve. Biomaterials, 2015, 37, 242-251.	11.4	186
9	Targeting tumour energy metabolism potentiates the cytotoxicity of 5-aminolevulinic acid photodynamic therapy. British Journal of Cancer, 2013, 109, 976-982.	6.4	44
10	Engineered neural tissue for peripheral nerve repair. Biomaterials, 2013, 34, 7335-7343.	11.4	185
11	Fully Protected Glycosylated Zinc (II) Phthalocyanine Shows High Uptake and Photodynamic Cytotoxicity in MCFâ€7 Cancer Cells. Photochemistry and Photobiology, 2013, 89, 139-149.	2.5	34
12	A 3D <i>in vitro</i> model reveals differences in the astrocyte response elicited by potential stem cell therapies for CNS injury. Regenerative Medicine, 2013, 8, 739-746.	1.7	15
13	Engineering an Integrated Cellular Interface in Three-Dimensional Hydrogel Cultures Permits Monitoring of Reciprocal Astrocyte and Neuronal Responses. Tissue Engineering - Part C: Methods, 2012, 18, 526-536.	2.1	19
14	Regulation of PP2A activity by Mid1 controls cranial neural crest speed and gangliogenesis. Mechanisms of Development, 2012, 128, 560-576.	1.7	18
15	Antioxidant Inhibitors Potentiate the Cytotoxicity of Photodynamic Therapy. Photochemistry and Photobiology, 2012, 88, 175-187.	2.5	64
16	Homing of stem cells to sites of inflammatory brain injury after intracerebral and intravenous administration: a longitudinal imaging study. Stem Cell Research and Therapy, 2010, 1, 17.	5.5	77
17	Alignment of Astrocytes Increases Neuronal Growth in Three-Dimensional Collagen Gels and Is Maintained Following Plastic Compression to Form a Spinal Cord Repair Conduit. Tissue Engineering - Part A, 2010, 16, 3173-3184.	3.1	100
18	A versatile 3D culture model facilitates monitoring of astrocytes undergoing reactive gliosis. Journal of Tissue Engineering and Regenerative Medicine, 2009, 3, 634-646.	2.7	90

Jon Golding

#	Article	IF	CITATIONS
19	Skeletal muscle stem cells express anti-apoptotic ErbB receptors during activation from quiescence. Experimental Cell Research, 2007, 313, 341-356.	2.6	60
20	Heparin-binding EGF-like growth factor shows transient left–right asymmetrical expression in mouse myotome pairs. Gene Expression Patterns, 2004, 5, 3-9.	0.8	17
21	Mouse myotomes pairs exhibit left-right asymmetric expression ofMLC3Fand α-skeletal actin. Developmental Dynamics, 2004, 231, 795-800.	1.8	15
22	Roles of erbB4, rhombomere-specific, and rhombomere-independent cues in maintaining neural crest-free zones in the embryonic head. Developmental Biology, 2004, 266, 361-372.	2.0	33
23	Myf5 expression in satellite cells and spindles in adult muscle is controlled by separate genetic elements. Developmental Biology, 2004, 273, 454-465.	2.0	61
24	Muscle satellite cells adopt divergent fates. Journal of Cell Biology, 2004, 166, 347-357.	5.2	779
25	Neural and mammary gland defects in ErbB4 knockout mice genetically rescued from embryonic lethality. Proceedings of the National Academy of Sciences of the United States of America, 2003, 100, 8281-8286.	7.1	227
26	ErbB4 Signaling During Breast and Neural Development: Novel Genetic Models Reveal Unique ErbB4 Activities. Cell Cycle, 2003, 2, 554-558.	2.6	20
27	Cues from neuroepithelium and surface ectoderm maintain neural crest-free regions within cranial mesenchyme of the developing chick. Development (Cambridge), 2002, 129, 1095-1105.	2.5	34
28	Cues from neuroepithelium and surface ectoderm maintain neural crest-free regions within cranial mesenchyme of the developing chick. Development (Cambridge), 2002, 129, 1095-105.	2.5	8
29	Defects in pathfinding by cranial neural crest cells in mice lacking the neuregulin receptor ErbB4. Nature Cell Biology, 2000, 2, 103-109.	10.3	162
30	A Two-Dimensional Gel Electrophoretic Study of Proteins Synthesized and Released by Degenerating Adult Mouse Sciatic Nerve. Experimental Neurology, 2000, 162, 194-200.	4.1	3
31	Behaviour of DRG sensory neurites at the intact and injured adult rat dorsal root entry zone: Postnatal neurites become paralysed, whilst injury improves the growth of embryonic neurites. Glia, 1999, 26, 309-323.	4.9	33
32	Chondroitin Sulphate-Binding Molecules May Pattern Central Projections of Sensory Axons within the Cranial Mesenchyme of the Developing Mouse. Developmental Biology, 1999, 216, 85-97.	2.0	27
33	Behaviour of DRG sensory neurites at the intact and injured adult rat dorsal root entry zone: postnatal neurites become paralysed, whilst injury improves the growth of embryonic neurites. Glia, 1999, 26, 309-23.	4.9	14
34	Border Controls at the Mammalian Spinal Cord: Late-Surviving Neural Crest Boundary Cap Cells at Dorsal Root Entry Sites May Regulate Sensory Afferent Ingrowth and Entry Zone Morphogenesis. Molecular and Cellular Neurosciences, 1997, 9, 381-396.	2.2	90
35	Effects of Extracellular Matrix Components on Axonal Outgrowth from Peripheral Nerves of Adult Animalsin Vitro. Experimental Neurology, 1997, 146, 81-90.	4.1	98
36	Maturation of the mammalian dorsal root entry zone- from entry to no entry. Trends in Neurosciences, 1997, 20, 303-309.	8.6	54

Jon Golding

#	Article	IF	CITATIONS
37	Anin VitroModel of the Rat Dorsal Root Entry Zone Reveals Developmental Changes in the Extent of Sensory Axon Growth into the Spinal Cord. Molecular and Cellular Neurosciences, 1996, 7, 191-203.	2.2	29
38	Expression of a developmentally regulated, phosphorylated isoform of microtubule-associated protein 1B in sprouting and regenerating axons in vitro. Neuroscience, 1996, 73, 541-551.	2.3	23
39	Cellular migration and axonal outgrowth from adult mammalian peripheral nervesin vitro. , 1996, 29, 151-164.		17
40	Protein Synthesis and Release by Normal and Lesioned Axolotl Peripheral Nerves. Experimental Neurology, 1995, 134, 94-101.	4.1	3
41	Oriented growth of regenerating axons in axolotl forelimbs is consistent with guidance by diffusible factors from distal nerve stumps. Neuroscience, 1995, 66, 201-213.	2.3	9
42	Early regeneration in vitro of adult mouse sciatic axons is dependent on local protein synthesis but may not involve neurotrophins. Neuroscience Letters, 1994, 168, 37-40.	2.1	19
43	Regeneration and repair of the peripheral nervous system. Seminars in Neuroscience, 1993, 5, 385-390.	2.2	15
44	Expression of GAP-43 in normal and regenerating nerves in the frog. Neuroscience, 1993, 52, 415-426.	2.3	11
45	Macrophage response during axonal regeneration in the axolotl central and peripheral nervous system. Neuroscience, 1993, 54, 781-789.	2.3	32
46	A study of the expression of laminin in the spinal cord of the frog during development and regeneration. Experimental Physiology, 1992, 77, 681-692.	2.0	6
47	Effects of freezing a segment of peripheral nerve on subsequent protein release and axonal regeneration in the frog. Experimental Neurology, 1992, 118, 178-186.	4.1	3
48	Regeneration in vitro of axolotl peripheral and central axons. Restorative Neurology and Neuroscience, 1990, 1, 267-273.	0.7	4